Low-Temperature Hydrogen Interaction with Amorphous Molybdenum Sulfides MoS x

ARTICLE *in* THE JOURNAL OF PHYSICAL CHEMISTRY C · DECEMBER 2009

Impact Factor: 4.77 · DOI: 10.1021/jp809300y

Low-Temperature Hydrogen Interaction with Amorphous Molybdenum Sulfides MoS_x

P. Afanasiev,*,† H. Jobic,† C. Lorentz,† P. Leverd,‡ N. Mastubayashi,§ L. Piccolo,† and M. Vrinat†

Institut de Recherche sur la Catalyse et Environnement, Université de Lyon 1, 69626, 2 avenue A. Einstein, Villeurbanne Cédex, France, Institut de Radioprotection et de Sûreté Nucléaire, B.P. 17, 92 262 Fontenay aux Roses, France, and National Institute of Advanced Industrial and Science Technology, Tsukuba Central 5, 1-1-1, Higashi, Tsukuba, Ibaraki 3058565, Japan

Received: October 21, 2008; Revised Manuscript Received: December 25, 2008

The low-temperature interaction of amorphous sulfur-rich sulfides MoS_3 and MoS_x ($x \approx 6$) with hydrogen was studied under static and dynamic conditions using volumetric measurements, mass spectrometry, solid-state NMR spectroscopy, inelastic neutron scattering, temperature-programmed reduction (TPR), and X-ray absorption spectroscopy (XAS) at the S K and Mo K edges. It was observed that, at room temperature, hydrogen irreversibly interacts with the sulfur species of the amorphous sulfide. Interaction with hydrogen leads to opening of the S—S bonds within the structure. As a result, SH groups are formed, which are very labile and are easily transformed into molecular H_2S under dynamic conditions (hydrogen flow). The total amount of absorbed hydrogen depends on the amount of S—S bonds in the amorphous sulfide, which can vary over a wide range.

1. Introduction

Interaction of sulfides with hydrogen has both fundamental and practical interest. In catalysis by sulfides, hydrogen activation is one of the key steps determining the catalytic performance of MoS_2-based catalysts, both unpromoted[1] and promoted.[2] Some data on the possibility of hydrogen storage by molybdenum sulfides have been published as well.[3] Many studies have focused on the interaction of H_2 with lamellar sulfides. Some of these compounds, such as NbS_2 and TaS_2,[4] can intercalate hydrogen within the layers, whereas others, such as MoS_2 and WS_2, do not intercalate any significant amounts between the layers but adsorb hydrogen on the surface, presumably at the edges. However, no data exist on the absorption of hydrogen by amorphous sulfides.

Recently, we studied the interaction of hydrogen with the amorphous cobalt oxysulfide material CoSOH.[5,6] It was demonstrated that amorphous CoSOH exposed to static hydrogen pressures can absorb large amounts of hydrogen. Volumetric measurements under static hydrogen pressure showed an intense H_2 absorption by the amorphous material, but the exact nature of the hydrogen species within the solid remained unclear. To provide additional insight into the reactivity of amorphous transition metal sulfides to hydrogen, more convenient model systems would be appropriate. This work considers the interaction between H_2 and the sulfur-rich molybdenum sulfides MoS_3 and MoS_{6-x}.

2. Experimental Techniques

To prepare the thiomolybdate precursors, high-purity starting materials were purchased from Sigma-Aldrich. Ammonium thiomonomolybdate $(NH_4)MoS_4$ was obtained by adding 15 g of $(NH_4)_6Mo_7O_{24}\cdot 4H_2O$ to 200 mL of a 20 wt % solution of $(NH_4)_2S$ at ambient temperature. The precipitated red crystals were thoroughly washed with small amounts of ethanol and tetrahydrofuran (THF) and then dried and stored under nitrogen. Ammonium thiodimolybdate $[(NH_4)Mo_2S_{12}]$ was prepared according to the literature method.[7] Molybdenum sulfides were prepared by acidification or oxidation with iodine of aqueous solutions of the corresponding thiometallates. In a typical preparation, 25 mL of 1 M HCl was rapidly added to a solution of 2.5 g of $(NH_4)_2MoS_4$ in 100 mL of water with vigorous stirring. The precipitate formed was washed with water, filtered, and dried in a strong flow of pure nitrogen for several days. Preparation of the sulfur-rich stoichiometric sulfide MoS_6 was described in our earlier work.[8]

A volumetric study of the solid—gas reaction was carried out in a vacuum glass system equipped with a pressure detector, as described earlier.[6] The X-ray diffraction patterns were obtained on a Bruker D5005 diffractometer with Cu Kα emission. The diffractograms were analyzed using the standard International Centre for Diffraction Data (JCPDS) files. Chemical analyses were performed using the atomic emission method on an inductively coupled plasma atomic emission spectrometer (SPECTROFLAME ICP model D). Prior to analysis, the solids were dissolved in HF acid. NMR spectra of protons in the solids were measured on an Avance DSX400 Bruker device, at 400 MHz frequency. Ex situ measurements were preformed in a sealed tube under 12 kHz magic angle spinning (MAS) rotation, whereas in situ measurements under hydrogen flow were carried out under static conditions.

Mo K-edge extended X-ray absorption fine structure (EXAFS) measurements were performed at the FAME X-ray beamline (ESRF, Grenoble, France) using a Si(111) monochromator. The measurements were carried out in transmission mode at the Mo K edge (20000 eV) at ambient temperature. The sample thickness was chosen to give an absorption edge step of about 1.0 near the edge region. Phase shifts and backscattering amplitudes were obtained from FEFF[9] calculations using the JCPDS structures of known solids such as MoS_2. The EXAFS

* Corresponding author. E-mail: pavel.afanasiev@ircelyon.univ-lyon1.fr.
† Université de Lyon 1.
‡ Institut de Radioprotection et de Sûreté Nucléaire.
§ National Institute of Advanced Industrial and Science Technology.

10.1021/jp809300y CCC: $40.75
Published on Web 02/12/2009

data were treated with the VIPER[10] program. The edge background was extracted using Bayesian smoothing with a variable number of knots. The curve fitting was done alternatively in R and k spaces. Coordination numbers (CNs), interatomic distances (R), Debye−Waller parameters (σ^2), and energy shifts (ΔE_0) were used as fitting variables. True Debye−Waller factors were determined by decorrelation from the coordination numbers as described previously.[11]

Neutron experiments were performed on the IN1BeF spectrometer, at the Institut Laue-Langevin, Grenoble, France. The INS spectra were measured from 240 to 2800 cm^{-1}. A beryllium filter was placed between the sample and the detector. This setting gives a moderate energy resolution, with an instrumental resolution varying from 25 cm^{-1} at small energy transfers to 50 cm^{-1} at large energy transfers. The frequency values were corrected from a systematic shift due to the beryllium filter. The estimated absolute accuracy is ~20 cm^{-1}. The spectra were recorded at 5 K to decrease the mean-square amplitude of the atoms and, thus, to sharpen the vibrational features.

The gaseous products evolved upon heating of the samples were studied using a mass spectrometer (Gas Trace A, Fison Instruments) equipped with a quadrupole analyzer (VG analyzer) working in a multiplier mode. The ionization was done by electron impact with an electron energy of 65 eV. The samples (ca. 0.1 g) were heated in a quartz cell at a heating rate of 5 K min^{-1}. A silica capillary tube heated at 453 K continuously bled off a portion of the gaseous reaction products.

S K-edge XAS measurements under hydrogen flow were carried out at Photon Factory (PF, Tsukuba, Japan) on the 9A soft X-ray beam line of PF. An in situ cell was constructed for these measurements, which included a sample holder, heater, and gas flow assembly. The in situ cell was installed in the measurement box flushed with helium to decrease the absorption soft X-rays. Spectra were collected in fluorescence mode. The real-space full-multiple-scattering ab initio code FEFF 8.2 was applied to simulate X-ray absorption near-edge structure (XANES) spectra and the pre-edge peaks with full-multiple-scattering (FMS) and self-consistent-field (SCF) radii between 4 and 5 Å. To simulate the structure of MoS_3 and MoS_6, the Mo−S neutral chainlike clusters Mo_6S_{19} and Mo_3S_{10} and the symmetric trimer Mo_3S_{13} cluster were used. Geometry optimization was first performed using molecular dynamics [calculations were performed using the Open Force Field (OFF) program in the Cerius^2 package (version 4.2)][12] and then refined using the PM6 parametrization level of the semi-empirical method implemented in the MOPAC 2007 software.[13]

Temperature-programmed reduction (TPR) was carried out in a quartz reactor. The samples of sulfides (ca. 0.005−0.05 g) were linearly heated under a hydrogen flow (10−50 cm^3 min^{-1}) from room temperature to 1373 K (1−10 K /min). Hydrogen sulfide evolved upon reduction was detected by means of an HNU photoionization detector equipped with a 10.2 eV UV light source. The amount of H_2S released from the solid was quantified after calibration of the detector with a gas mixture of known H_2S content.

3. Results and Discussion

Earlier, we studied room-temperature H_2 interaction with the amorphous cobalt oxysulfide "CoSOH".[5,6] This solid, obtained from the precipitation of cobalt soluble salts and sodium sulfide solutions, is an ill-defined amorphous and nonstoichiometric compound. Several characterizations supported the hypothesis of the formation of SH groups after hydrogen absorption by this solid. However, the evidence was not straightforward because it was entirely based on difference INS spectra and a change in shoulder intensity in a Raman spectrum. Moreover, the presence of a $Co(OH)_2$ impurity phase in the CoSOH material introduced additional complications to the data interpretation, because cobalt hydroxide can react with the sulfhydride species or hydrogen sulfide. Amorphous molybdenum sulfides, although also nonstoichiometric, are much better known, as many works have focused on the MoS_3 amorphous sulfide, which is assumed to be an intermediate phase in hydrotreating catalysts.[14]

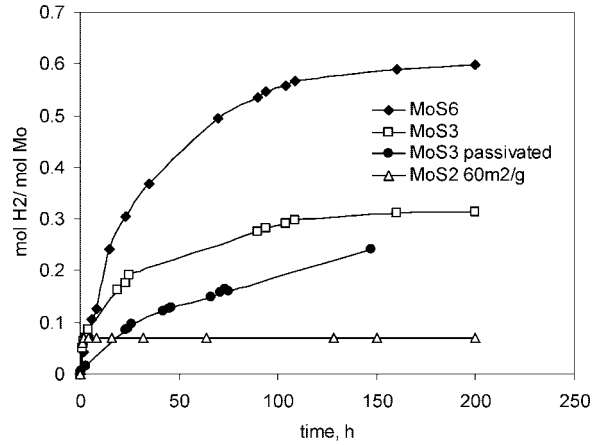

Figure 1. Absorption of H_2 under static conditions by sulfur-rich molybdenum sulfides and highly dispersed MoS_2.

3.1. Volumetric Measurements. The stoichiometry and kinetics of hydrogen sorption by MoS_3 and MoS_6 were studied using a constant-volume glass system. The large excess of hydrogen used in our experiments and the relatively small drop in H_2 pressure (i.e., from 580 to 540 mbar for the MoS_3 reaction with hydrogen) allowed for the assumption of local linearity of the reaction rate as a function of H_2 pressure (although, in general, there is obviously no such linearity).

After being dried under an inert gas flow, MoS_3 is pyrophoric when exposed to air. (*Caution: Rapid exposure of large quantities of MoS_3 to air can cause fire.*) To avoid the possibility of fire, the solid was first passivated by exposing it to a flow of 1% O_2 in Ar. However, passivated samples had low and poorly reproducible H_2 absorbing capacities and demonstrated complex kinetic behavior, as seen in Figure 1. Therefore, we replaced passivation by loading of the wet solid into the volumetric cell with further prolonged evacuation to a vacuum of $<10^{-3}$ mbar. The amorphous molybdenum sulfide obtained after the sample had been dried in a vacuum for 48 h at room temperature, designated in this work as "MoS_3", had the chemical formula $MoS_{3.02}N_{0.03}O_{0.02}H_{0.14}$. Nitrogen was present probably because of residual ammonium ions from the parent ammonium thiomolybdate. This nitrogen was hard to wash out; therefore, it seems to be deeply occluded within the solid. Oxygen was present because of residual moisture. Residual hydrogen was distributed between ammonium ions, moisture, and perhaps some SH groups. The presence of such impurities is inevitable for amorphous MoS_3 prepared by means of aqueous chemical precipitation.

As follows from the volumetric experiments, MoS_3 absorbs up to 0.3 mol of hydrogen per mole of Mo. Sulfur-rich MoS_6 sulfide showed a molar capacity nearly twice that of MoS_3, probably because it provides more sulfur species to react, whatever their exact nature. MoS_6 demonstrated process kinetics very similar to that of MoS_3, suggesting that the two sulfides have similar types of reacting moieties but different amounts

of them. Analysis of conversion-rate curves showed that the absorption kinetics for both MoS_6 and MoS_3 followed a first-order rate law with respect to the nonreacted compound. Therefore, for the dried sulfides, only the chemical gas−solid interaction seems to determine the process kinetics. The interaction obviously occurs without any nucleation- or diffusion-related slow steps. By contrast, the passivated sample of MoS_3 showed hydrogen absorption kinetics that could not be described by any simple kinetics law. After the initial decrease of the rate, MoS_3 absorbed hydrogen almost linearly, as if a constant bottleneck appeared as a result of the passivation. Further study of this curious finding was beyond the scope of this work. A striking difference was observed between the kinetics of absorption by amorphous sulfides and dispersed MoS_2 (surface area = 57 m^2/g). The latter solid absorbed ca. 0.07 mol of H_2/mol of Mo and attained saturation at this point within several minutes. Therefore, only chemisorption at the available surface sites probably occurs for MoS_2, as opposed to slow processes observed for the amorphous sulfides.

In summary, the volumetric study demonstrated that, unlike dispersed crystalline MoS_2, amorphous molybdenum sulfides can absorb significant amounts of hydrogen at ambient temperature. In the case of MoS_3, this amount corresponds to a final stoichiometry $MoS_{3.02}N_{0.03}O_{0.02}H_{0.64}$. A striking similarity to the previously observed slow hydrogen absorption by solid CoSOH leads to the conclusion that the natures of the reacting species should be similar. Moreover, even the time scales observed in the two cases were quite close (150−200 h under H_2 pressure of 500−700 mbar). It appears that the reacting species are the same (presumably S−S bonds), whereas the nature of the transition metal is less important for the reactivity.

3.2. ^{1}H NMR Spectra. In situ solid-state NMR spectroscopy of protons in the MoS_3 solid was carried out under hydrogen flow at room temperature and 373 K. In these experiments, we expected to see an increase of some signal corresponding to the stored hydrogen and thus to identify the form in which hydrogen accumulated in the solid. The initial dried MoS_3 specimen showed a weak signal with two components at 7.8 and 4.2 ppm, as well as a shoulder at 2.4 ppm, corresponding to ammonium ions, residual moisture, and SH species, respectively.[15] Under a hydrogen flow at room temperature or 373 K, there was no formation of any new hydrogen species detectable by NMR spectroscopy (Figure 2a). Only a decrease of the moisture signal was observed, whereas the signal attributed to ammonium species remained unchanged. Therefore, the behavior of MoS_3 solid under hydrogen flow is seemingly contradictory to the significant hydrogen absorption observed by volumetric measurements. However, the absence of any increasing H-species signals can be also explained by the eventual formation of paramagnetic species. If H_2 absorption is related to Mo reduction and formation of concomitant paramagnetic centers, then the signal of the corresponding protons would be hardly observable because of the interaction with electron spin. Indeed, some line broadening was clearly observed for the signal of the hydrogen-treated sample, as compared to the initial one (Figure 2b).

3.3. Inelastic Neutron Scattering (INS) Study. For the amorphous molybdenum sulfides, conventional vibrational spectra are difficult to obtain because the solids are black in the IR region and fragile in the Raman spectrometer laser beam, rapidly transforming to MoS_2 slabs under inert atmosphere and even more rapidly burning in air to give MoO_3, even at low laser power. By contrast, INS allows selective detection of vibrations related to the protons in solids. To rule out the uncertainty of NMR analysis concerning the nature and respective amounts of the protons, INS is the technique of choice, as the cross section of scattering is the same for different vibrational modes. Therefore, integration of the fundamental vibrations peaks allows for a comparison of the amounts of protons, whatever their chemical nature.

Previously, hydrogen adsorption by microcrystalline molybdenum sulfide was studied using INS.[16] These works showed agreement on the attribution of main peak near 700 cm^{-1} (85 meV) to the bending of S−H groups. First, the harmonic of this vibration is observed at twice the frequency. Adsorption of hydrogen on the ruthenium sulfide RuS_2, which contains $S-S^{2-}$ ions, has also been studied by this technique, and opening of S−S bonds was suggested to be the main sorption mechanism.[17] Two nondegenerate S−H bending modes at 600 and 710 cm^{-1} were observed.

In the initial and treated samples (Figure 3), the same set of broad peaks was observed at 45, 53, 87, 159, and 179 meV (367, 427, 701, 1283, and 1459 cm^{-1}, respectively). Previous literature assignments were used to analyze these spectra. First, there is no molecular water in the samples because wagging and twisting modes should arise simultaneously between 55 and 71 meV, whereas the rocking band is situated between 73 and 78 meV and the deformation is at 200 meV.[18] However, the presence of some OH groups cannot be excluded. Neither bonded ammonia nor NH_2 groups can be present, but ammonium ions would account for the peak at 180 meV. Indeed, bending modes near 180 meV and libration at 40 meV were observed previously for ammonium ions in Y zeolite.[19]

The intensity below 400 cm^{-1} (50 meV) is difficult to interpret because it is poorly resolved and might contain contributions from hydrogen-coupled lattice vibrations. However, if we assume that hydroxide librations are observed near 50 meV, then the decrease of this peak suggests that further removal of hydroxide traces from the sample occurred under hydrogen flow. This conclusion agrees with other characterizations. The total amount of protons in the sample decreases after hydrogen treatment, whereas the relative amount of SH groups somewhat increases. The intensity of the 180 meV peak does not change upon hydrogen treatment, which supports the supposition that it is due to ammonium ions.

Overall, the INS study showed that no new species appear in the amorphous sulfide upon room-temperature hydrogen flow treatment, but a slight increase of the relative proportion of SH groups occurs. Again, no hydrogen storage can be inferred from the INS study, in contrast to the volumetric data.

3.4. XAS Study. The X-ray diffraction patterns of MoS_3 and MoS_6 before and after their interaction with hydrogen corresponded to completely amorphous solids (not shown). X-ray absorption spectroscopy (XAS) is the method of choice for studying the evolution of coordination in such amorphous solids. To follow the states of the constituent elements and their evolution during the interaction with hydrogen, XAS at the Mo K and S K edges was measured under ex situ and in situ conditions.

3.4.1. S K-Edge XAS Spectra. Initial and hydrogen-treated MoS_3 specimens were compared at the S K edge with each other and with the MoS_2 references. Usually, on the basis of the S K-edge EXAFS part of spectra, the distances in the first shell can be fitted, with a satisfactory correspondence of fitted distances with the known values for the crystalline references. Unfortunately, this is not the case for molybdenum sulfides, where the range of k values available for fitting the S K-edge spectra is too small because of the closeness of the S K

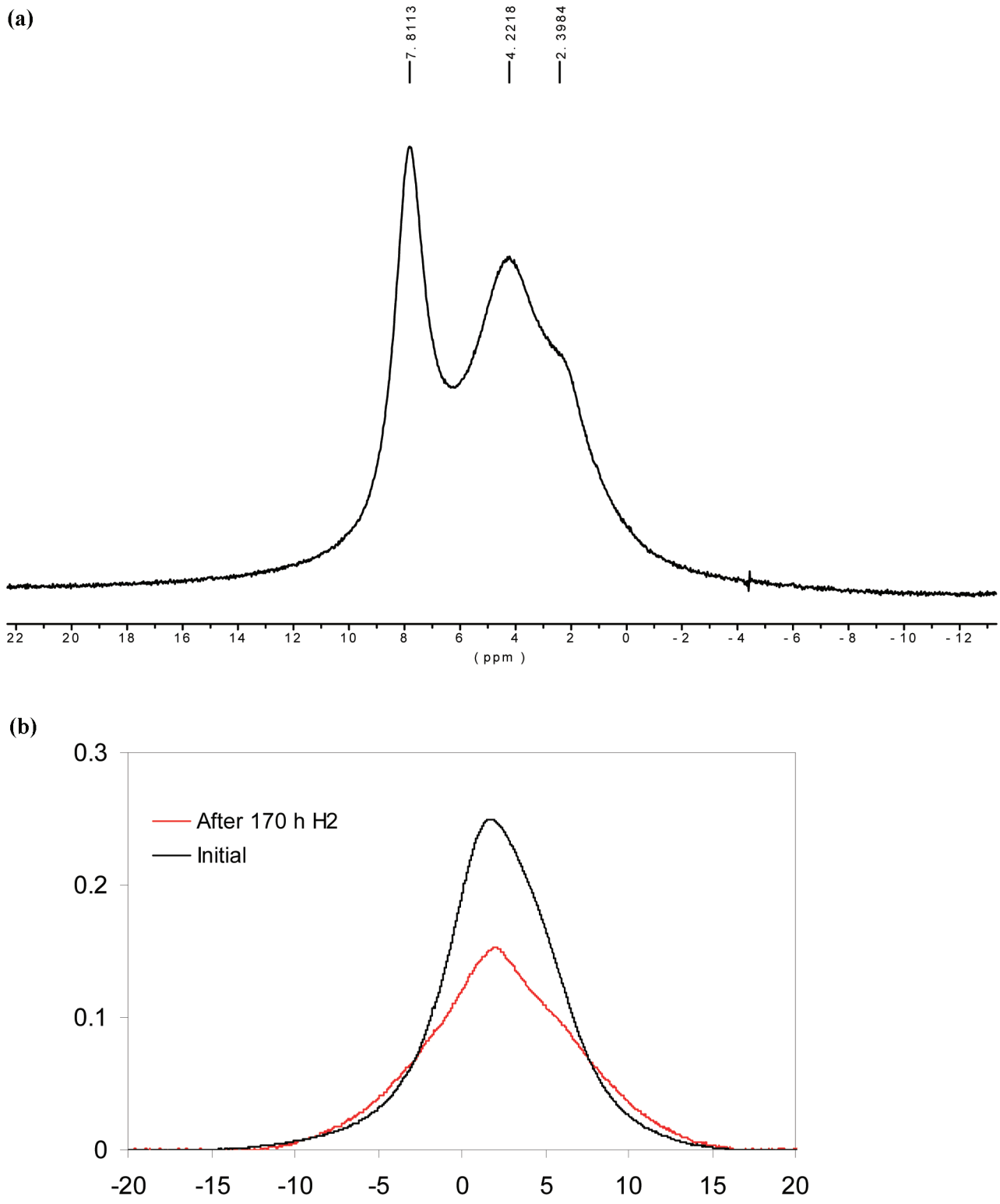

Figure 2. (a) MAS 10 kHz ^{1}H NMR spectrum of MoS_3 after 170 h under H_2 flux. (b) Static ^{1}H NMR spectra of MoS_3 before treatment and after 170 h under H_2 flux.

(2472 eV) and Mo L_{III} (2520 eV) edges (the latter gives a strong negative intensity in the very beginning of EXAFS part of the spectra). That is why Hibble et al. reported on EXAFS at the S K edge of tungsten and rhenium amorphous sulfides, but not those of molybdenum.[20] Therefore, we focused on an analysis of the near-edge X-ray absorption fine structure (NEXAFS) part of the spectra for fingerprint characteristics of the sulfur species in the amorphous sulfide.

XANES at the S K edge of MoS_3 showed a distinct absorption jump at 2470.6(2) eV; that of the MoS_2 reference was observed at 2469.8(2) eV. Because of the high resolution at the S K edge, this difference can be considered as significant (Figure 4a). Ab initio simulation (vide infra) gives values of 2470.4 for MoS_3 (Mo_3S_{10} cluster) and 2469.5 eV for MoS_2. Qualitative analysis of the profile shapes showed a striking difference between the amorphous sulfide and MoS_2 (Figure 4b). Note that finely di-

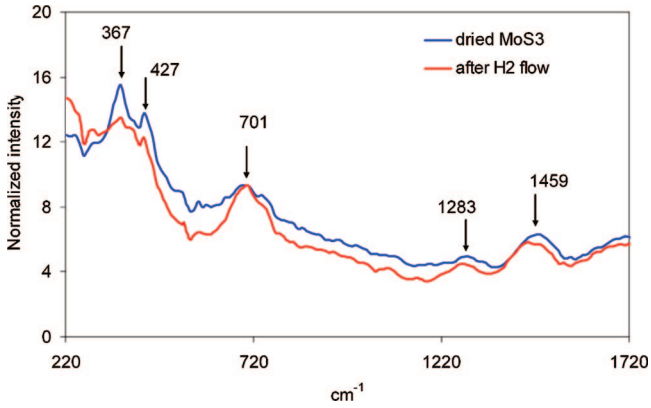

Figure 3. INS spectra of MoS_3 before treatment and after 170 h under hydrogen flow at room temperature.

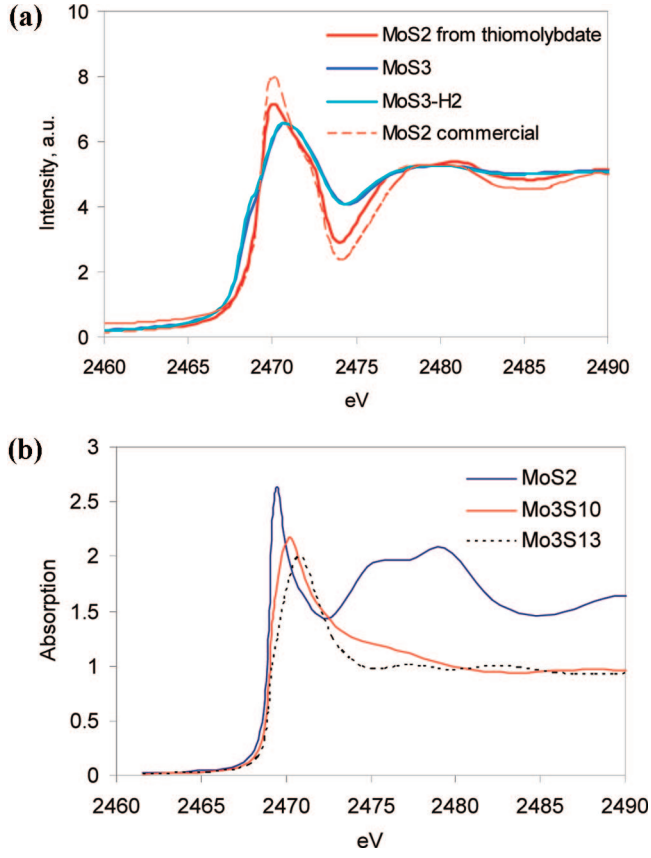

Figure 4. (a) S K-edge spectra of MoS_3 before treatment and after 170 h under H_2 flow at room temperature, commercial MoS_3 powder, and dispersed MoS_2 obtained from the decomposition of ammonium thiomolybdate at 673 K. (b) FEFF 8 simulations of the S K-edge NEXAS part of molybdenum sulfide and clusters modeling possible MoS_3 structures.

vided MoS_2 demonstrated somewhat broader and less intense features than the commercial bulk reference sulfide. However, their spectra were similar and qualitatively different from the MoS_3 spectra. The higher energy of the absorption edge of MoS_3 compared to MoS_2 corresponds to the expected increase in the oxidation state of sulfur (from 2− in MoS_2 to intermediate between 2+ and 1− in MoS_3). FEFF 8 simulations showed good correspondence of the edge shape with the nature of the sample. No pre-edge features were observed in agreement with FEFF simulation results. As follows from the S K-edge XANES profiles, the coordination of sulfur was not changed as a result of the interaction with hydrogen for 170 h. Only a very slight

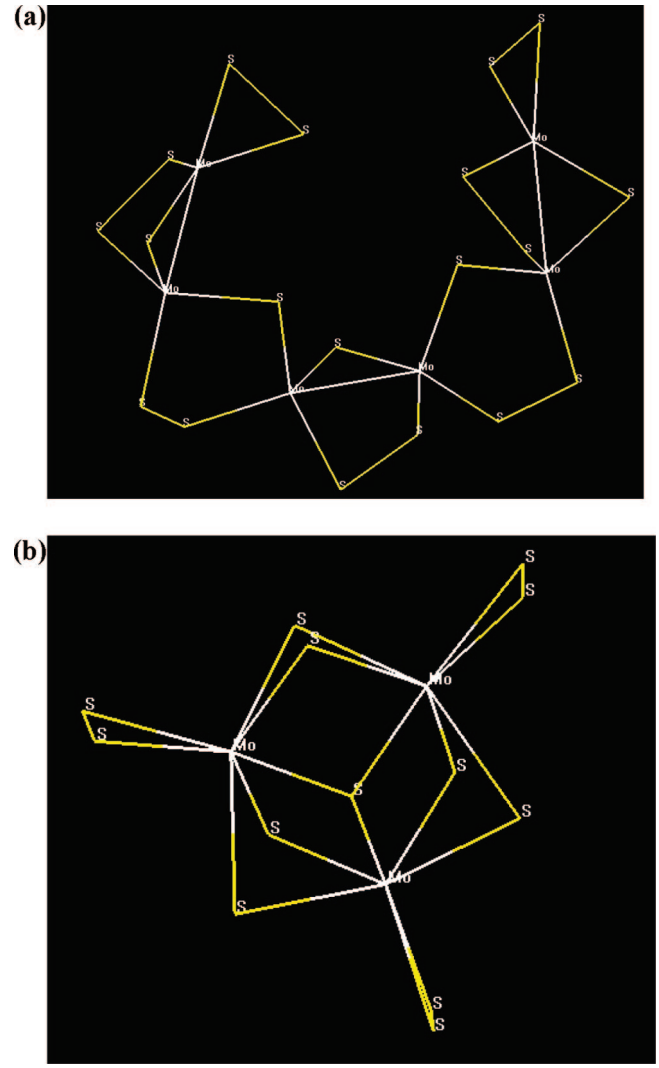

Figure 5. (a) Optimized Mo_6S_{19} cluster used for the simulations of properties of amorphous MoS_3 sulfide. (b) Optimized structure of the Mo_3S_{13} trimeric cluster used for ab initio simulations.

increase in the low-frequency shoulder could be detected. Any reduction or structural change with formation of MoS_2 can therefore be ruled out. Again, this seems surprising taking into account the great amount of hydrogen that can be absorbed by the amorphous sulfide.

3.4.2. Mo K-Edge XANES and EXAFS. As shown by earlier EXAFS studies at the Mo K edge, in amorphous MoS_3, the coordination of molybdenum is strikingly different from that in the crystalline structure MoS_2. Both the number of neighbors and the Mo—S and Mo—Mo distances are considerably different.[21] Therefore, formation of MoS_2 through reduction by hydrogen, even if this sulfide were disordered and very poorly crystalline, would in any case be immediately seen because of its specific XAS signature. Although it is obvious that the MoS_3 structure is not similar to that of MoS_2, the exact structure of MoS_3 is much less clear and has been the subject of debate (see the review in ref 22 and references therein). The chainlike structure and the Mo_3S_{13} trimer-based structure were proposed as alternative models. Both of them coherently explain the majority of the properties of these sulfides.[23]

As shown by ab initio simulations of the XANES spectra, better correspondence of XANES profile to the experimental data for MoS_3 is achieved in the case of the chainlike clusters Mo_3S_{10} and Mo_6S_{19} (Figure 5a) rather than the trimeric Mo_3S_{13}

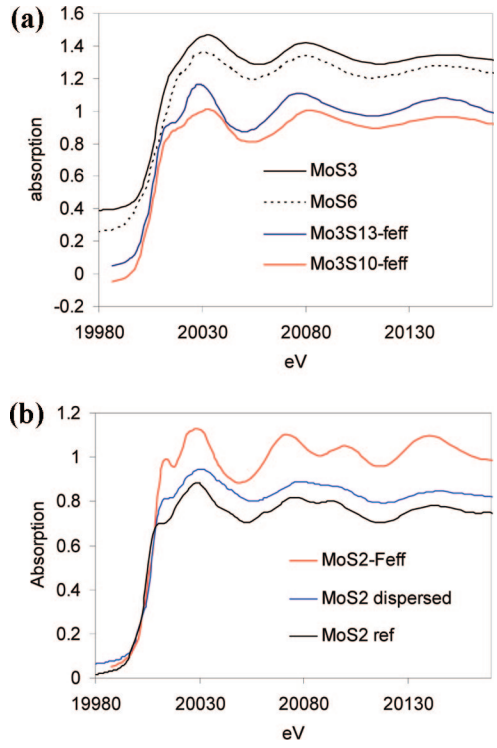

Figure 6. (a) Mo K-edge XAS spectra of amorphous sulfides and FEFF 8 simulations based on the chainlike and trimeric structure guesses. (b) Mo K-edge XAS spectra of the MoS_2 commercial reference and highly dispersed MoS_2 and FEFF 8 simulation based on the MoS_2 structure.

(Figure 5 b). This cannot be considered as decisive evidence but clearly supports the chain model. As follows from the striking similarity of MoS_3 and MoS_6 spectra, a chainlike type of structure is probably common for MoS_3 and other sulfur-rich sulfides, which should differ in just the number of connecting S—S bonds. It is worth emphasizing that, both in the experiments and in the ab initio simulations, addition (or removal) of extra sulfur as new S—S bonds did not significantly affect the shape of the spectra (Figure 6). Similar results were obtained as well using the Mo_3S_{10} cluster and the twice larger Mo_6S_{19} cluster, which is a consequence of the rapid decrease in the amplitude of scattering paths with increasing length.

Again, as in the case of the S K edge, qualitative and quantitative analyses of spectra before and after interaction with hydrogen do not reveal any differences in the coordination type of molybdenum. However, in this case, a non-negligible difference in coordination numbers was detected. Analysis of the MoS_6 EXAFS spectra showed that the coordination number decreases as a result of interaction with hydrogen, whereas the material remains amorphous and keeps the same distance to sulfur neighbors and the same number of second Mo neighbors. To calibrate this amplitude attenuation factor, bulk crystalline MoS_2 was applied as a reference. A high-fidelity fit was obtained with an R factor of less than 3%, allowing quite reliable values to be obtained (Table 1). It can be seen that interaction with a hydrogen flow for 170 h removes roughly two of every seven sulfur atoms from the coordination sphere of molybdenum in the MoS_6 sample. A similar but smaller effect was observed for MoS_3. Note that the mean coordination number does not necessarily change in step with the sulfur content in the solids, but rather depends on the topology of connectivity. However, it can be speculated that, if sulfur is removed without any structural reorganization of the solid (probable at room temperature), then some regular decrease of the apparent coordination number should be observed.

TABLE 1: Mo K-Edge EXAFS Fitting Results for the Amorphous Molybdenum Sulfides before and after Interaction with Hydrogen (170-h Flow at Room Temperature)[a]

	R (Å)	CN	σ^2 (Å^2)	ΔE (eV)	R (%)
Initial MoS_6					
S	2.447(5)	6.9(1)	0.0053(6)	2.8	3.2
Mo	2.785(5)	1.3(1)	0.0028(3)	1.2	
MoS_6 after Interaction with H_2 at Room Temperature					
S	2.441(5)	6.0(1)	0.0052(6)	3.6	3.7
Mo	2.779(6)	1.3(1)	0.0030(4)	3.0	
Initial MoS_3					
S	2.435(5)	5.8(5)	0.0058(5)	2.5	4..2
Mo	2.771(5)	0.9(1)	0.0041(4)	2.8	
MoS_3 after Interaction with H_2 Flow					
S	2.429(5)	5.4(5)	0.0065(5)	3.3	5.1
Mo	2.762(6)	0.9(1)	0.0038(4)	3.0	
MoS_2 Crystalline Reference					
S	2.402(1)	6.02(8)	0.0027(1)	3.5	2.1
Mo	3.159(1)	6.85(5)	0.0031(2)	2.6	

[a] From the analysis of crystalline reference, a value for the amplitude attenuation factor S_0^2 of 0.89 was found. All fitting variables were freely varied, without any constraints.

3.5. Mass Spectra of the Evolved Gases. Chemical analysis shows that MoS_3 dried under nitrogen flow or in a vacuum at room temperature still contains protons, namely, small amounts occluded moisture and residual ammonium species, as well as SH groups. As expected from the chemical composition, heating of the initial MoS_3 solid under inert gas flow leads to the release of water, ammonia, and hydrogen sulfide (Figure 7a). A considerable amount of elemental sulfur is deposited on the cold parts of the reactor as a result of the decomposition of MoS_3 and formation of MoS_2. This sulfur does not reach the mass spectrometer, and therefore, no release of sulfur was observed in the mass spectra. The most significant part of the protons is released as water. However, this does not mean that they must be present as OH groups, as proton exchange during heating might be intense. The relatively high temperature for ammonia formation confirms that the nitrogen-containing species are ammonium ions, probably issued from the parent thiomolybdate. Indeed, the high temperature of ammonia release corresponds to the decomposition of chemically bonded species rather than desorption of the adsorbed ammonia. Moreover, the solid obtained from the initial sample after an additional 3 days of drying under nitrogen showed the same signal of NH_3 but much less hydrogen sulfide and water (Figure 7c).

Another measurement was carried out on the same sample after its treatment at room temperature under hydrogen flow for 16 h. The mass spectrum was only slightly affected, with the low-temperature part of H_2S broad peak being decreased. MoS_2 was obtained as a result of decomposition of amorphous sulfides above 400 °C, in agreement with a previous thermal analysis study.[24]

As a conclusion of the MS study, no significant amounts of hydrogen were desorbed by the solid after its treatment under hydrogen flow. Therefore, no reversible storage of hydrogen is possible by amorphous molybdenum sulfide. Nor was any increase in the amounts of hydrogen-containing molecules observed. All of the characterizations then coherently indicate that hydrogen (in any form) is not kept within the solid under dynamic conditions.

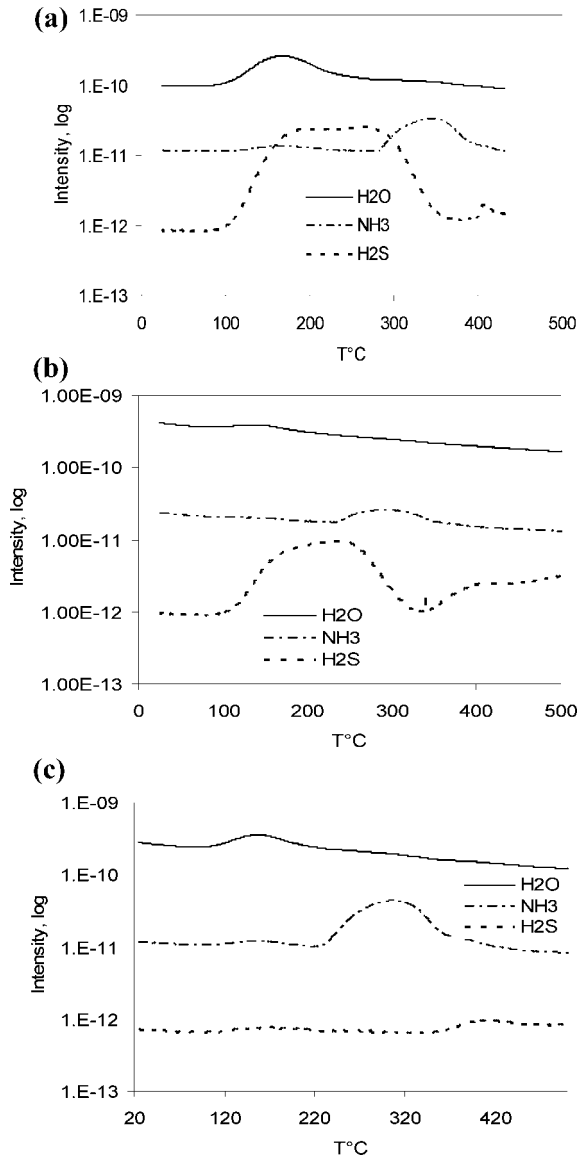

Figure 7. Mass spectrometric signals of gases evolved upon linear heating of MoS_3 under inert gas flow: (a) initial MoS_3, (b) after 16 h under hydrogen, (c) after additional 72 h under nitrogen.

3.6. Temperature-Programmed Reduction (TPR). Previous characterizations showed that the interaction of MoS_x sulfides with hydrogen seems to be just an unusually easy reduction. The characterization technique used to straightforwardly verify this point is TPR. In the temperature-programmed reduction (TPR) study, we selectively detected gaseous H_2S evolving from the solids upon linear heating under hydrogen flow. It appears that both amorphous sulfides give a strong peak at low temperatures with a maximum near 150 °C. For the MoS_6 sulfide, the area of this peak is expectedly much higher than for the MoS_3 one (Figure 8). Such a low-temperature peak is very small or absent in the TPR of dispersed MoS_2 obtained from thiomolybdate decomposition. At higher temperatures, all sulfides show the same exponentially growing signal corresponding to an equilibrium amount of H_2S with the nonreduced sulfide. This branch was called thermodynamic TPR peak because it corresponds to the thermodynamic equilibrium and the heat of sulfide formation can be extracted from it under appropriate experimental conditions.[25]

The TPR experiments are complimentary to the mass spectrometric study, providing similar information. However, the sensitivity of the method is at least 2 orders of magnitude higher, and the quantitative analyses are more accurate. Note that the mass spectra were detected during heating of the solid after the interaction with H_2 to study desorped species, whereas TPR measures hydrogen sulfide produced during the solids' interaction with H_2 (but at a much shorter time scale).

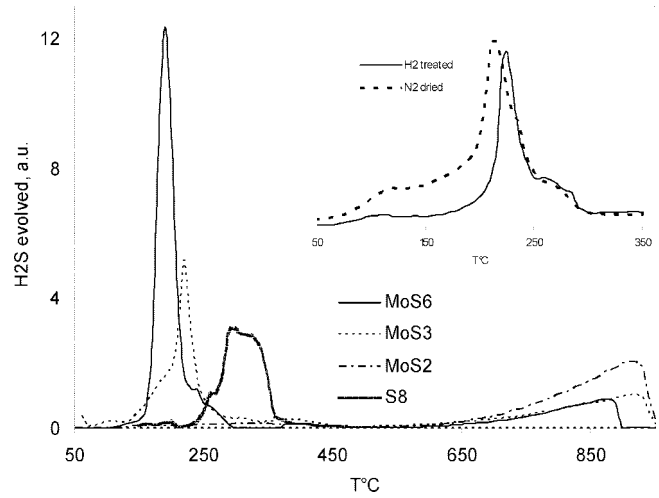

Figure 8. TPR curves of the amorphous molybdenum sulfides, dispersed MoS_2 reference, and elemental sulfur impregnated on γ-alumina (specific surface area = 200 m^2/g). Inset: Low-temperature part of TPR curves for nitrogen-dried and hydrogen-treated MoS_3.

The TPR results suggest that the reduction of amorphous sulfides might have non-negligible rate even at room temperature. A rough qualitative analysis can be presented to support the idea that the low-temperature peak corresponds to the same process as observed in volumetric measurements at room temperature. Indeed, the process of reduction at room temperature or at 50 °C requires several days or weeks, whereas the onset of the intense reduction in TPR occurs at about 110−130 °C and takes several minutes. The time scale therefore differs by approximately 2^{10}. For an activated process with a typically observed activation energy of a few tens of kilojoules per mole, the rate is doubled every 10 or 15 °C. Therefore, the difference in time scale of 2^{10} corresponds approximately to a temperature difference of about 100−150°, just as observed in our experiments. Note that only the S−S groups bonded to a transition metal (Mo) show such reactivity, whereas the S−S bridge in elemental sulfur does not. Indeed, S_8 impregnated on alumina gave a reduction peak at much higher temperatures (Figure 8). Finally, TPR gives quite straightforward evidence of removal of the weakly bonded sulfur at low temperature. Comparison of the TPR patterns of the MoS_3 samples before and after low-temperature interaction with hydrogen shows that the first TPR peak decreases considerably and shifts to somewhat higher temperatures as a result of the exposure to hydrogen flow at ambient temperature (see inset in Figure 8).

4. Conclusions

A coherent picture of the MoS_x ($x > 3$) interaction with hydrogen was obtained from this study, which also fully explains previously obtained data on the similar cobalt system and probably extends to other amorphous sulfides containing S−S bonds. Unlike the oxides (e.g., molybdenum bronzes[26]), hydrogen can be dissociated on the surface and reduces sulfides even at low temperatures without any hydrogen activator. This hydrogen cannot be reversibly desorbed. Under static conditions, it probably remains as HS− groups or molecular H_2S absorbed within the solid. However, under a hydrogen flow it is rapidly removed.

In other words, in the sequence

$$\text{Mo—S—S—Mo} \rightarrow 2\text{MoSH} \rightarrow \text{MoS—Mo—SH}_2 \quad (1)$$

the first step is obviously slow compared to the second one. Interaction with hydrogen occurs over days and weeks, whereas no convincing evidence could be obtained for the presence of any considerable amounts of the stable intermediate —SH moieties within the solid. The high lability of vicinal —SH groups produced by the S—S bonds opening, following from these data, provides additional insight into the problem of hydrogen activation by layered MoS_2. It has been suggested that S—S bridges are the species that generate active SH groups in the sulfide catalysts. It follows from our data that the S—S bridges are readily opened by hydrogen, even at relatively low temperatures.

Acknowledgment. The authors gratefully acknowledge Dr. Alexander Ivanov (instrument responsible of IN1BeF at the Institut Laue-Langevin, Grenoble, France) and Dr. Olivier Proux (BM30 beamline at the ESRF, Grenoble, France). The S K-edge XAFS measurements were done under the approval of the Photon Factory Advisory Committee (No. 2006G126).

References and Notes

(1) (a) Paul, J. F.; Cristol, S.; Payen, E. *Catal. Today* **2008**, *130*, 139. (b) Hinnemann, B.; Moses, P. G.; Bonde, J.; Jorgensen, K. P.; Nielsen, J. H.; Horch, S.; Chorkendorff, I.; Norskov, J. K. *J. Am. Chem. Soc.* **2005**, *127*, 5308.

(2) (a) Zuo, D.; Li, D.; Nie, H.; Shi, Y.; Lacroix, M.; Vrinat, M. *J. Mol. Catal. A.* **2004**, *211*, 179. (b) Rodriguez, J. A. *J. Phys. Chem. B.* **1997**, *101*, 7524.

(3) (a) Chen, J.; Kuriyama, N.; Yuan, H.; Takeshita, H. T.; Sakai, T. *J. Am. Chem. Soc.* **2001**, *123*, 11813. (b) Chen, J.; Li, S. L.; Tao, Z. L. *J. Alloys Compd.* **2003**, *356*−*357*, 413.

(4) Makara, V. A.; Babich, N. G.; Zakharenko, N. I.; Pasichnyi, V. A.; Rudenko, O. V.; Surzhko, V. F.; Kulikov, L. M.; Semenov Kobzar, A. A.; Antonova, M. M.; Akselrud, L. G.; Romaka, L. P. *Inorg. Mater.* **1997**, *33*, 1113.

(5) Loussot, C.; Pichon, C.; Afanasiev, P.; Vrinat, M.; Pijolat, M.; Valdivieso, F.; Chevarier, A.; Millard-Pinard, N.; Leverd, P. C. *J. Nucl. Mater.* **2006**, *359*, 238.

(6) Loussot, C.; Afanasiev, P.; Vrinat, M.; Jobic, H.; Leverd, P. C. *Chem. Mater.* **2006**, *18*, 5659.

(7) McDonald, J. W.; Friesen, G. D.; Rosenhein, L. D.; Newton, W. E. *Inorg. Chim. Acta* **1983**, *72*, 205.

(8) Afanasiev, P.; Bezverkhyy, I. *Chem. Mater.* **2002**, *14*, 2826.

(9) Rehr, J. J.; Zabinsky, S. I.; Albers, R. C. *Phys. Rev. Lett.* **1992**, *69*, 3397.

(10) Klementiev, K. V. *J. Phys. D: Appl. Phys.* **2001**, *34*, 209.

(11) Genuit, D.; Afanasiev, P.; Vrinat, M. *J. Catal.* **2005**, *235*, 302.

(12) *Cerius2*; Molecular Simulation Inc.: San Diego, CA, June 2000.

(13) Stewart, J. J. P. *MOPAC2007*, ver. 7.065W; Stewart Computational Chemistry: Colorado Springs, CO, 2007.

(14) Ratnasamy, P.; Léonard, A. J. *J. Catal.* **1972**, *26*, 352.

(15) Lindner, E.; Dreher, H. *J. Organomet. Chem.* **1973**, *55*, 347.

(16) (a) Wright, C. J.; Sampson, C.; Fraser, D.; Moyes, R. B.; Wells, P. B.; Riekel, C. *J. Chem. Soc., Faraday Trans. 1* **1980**, *76*, 1585. (b) Lacroix, M.; Jobic, H.; Dumonteil, C.; Afanasiev, P.; Breysse, M.; Kasztelan, S. *Stud. Surf. Sci. Catal.* **1996**, *101*, 117.

(17) Heise, W. H.; Lu, K.; Kuo, Y. J.; Udovic, T. J.; Rush, J. J.; Tatarchuk, B. J. *J. Phys. Chem.* **1988**, *92*, 5184.

(18) Plazanet, M.; Glaznev, I.; Stepanov, A. G.; Aristov, Yu., I.; Jobic, H. *Chem. Phys. Lett.* **2006**, *419*, 111.

(19) (a) Jobic, H.; Lacroix, M.; Decamp, T.; Breysse, M. *J. Catal.* **1995**, *157*, 414. (b) Jacobs, W. P. J. H.; Van Santen, R. A.; Jobic, H. *J. Chem. Soc., Faraday Trans.* **1994**, *90*, 1191.

(20) Hibble, S. J.; Walton, R. I.; Feaviour, M. R.; Smith, A. D. *J. Chem. Soc., Dalton Trans.* **1999**, 2877.

(21) Walton, R. I.; Dent, A. J.; Hibble, S. J. *Chem. Mater.* **1998**, *10*, 3738.

(22) Afanasiev, P. *C. R. Chim.* **2008**, *11*, 159.

(23) (a) Hibble, S. J.; Rice, D. A.; Pickup, D. M.; Beer, M. P. *Inorg. Chem.* **1995**, *34*, 5109. (b) Hibble, S. J.; Walton, R. I.; Pickup, D. M.; Hannon, A. C. *J. Non-Cryst. Solids* **1998**, *232*, 434. (c) Muller, A.; Fedin, V.; Hegetschweiler, K.; Amrein, W. J. *J. Chem. Soc., Chem. Commun.* **1992**, 1795. (d) Hibble, S. J.; Feaviour, M. R.; Almond, M. J. *J. Chem. Soc., Dalton Trans.* **2001**, 935.

(24) Brito, J. L.; Iljia, M.; Hernandez, P. *Thermochim. Acta* **1995**, *256*, 325.

(25) Afanasiev, P. *Appl Catal.* **2006**, *303*, 110.

(26) Noh, H.; Wang, D.; Luo, S.; Flanagan, T. B.; Balasubramaniam, R.; Sakamoto, Y. *J. Phys. Chem. B* **2004**, *108*, 310.

JP809300Y